ESA RFP/3-17035/20/NL/FF/tfd

NGGM/MAGIC – Phase A Extension of Science Support Study during Phase A – Executive Summary

In November 2020 it was decided at ESA's Ministerial Conference to investigate a European next-generation gravity mission (NGGM) in Phase A as first Mission of Opportunity in the FutureEO Programme. The Mass-change And Geoscience International Constellation (acronym: MAGIC) is a joint investigation with NASA's MCDO study resulting in a jointly accorded Mission Requirements Document (MRD 2020) responding to global user community needs. The MAGIC mission will be composed of two pairs flying in different orbit planes. As baseline assumptions at the current stage of NGGM Phase A, the NASA/DLR–developed first pair (P1) of MAGIC will be in a near-polar orbit at altitude around 500 km, while the ESA–developed second pair (P2) NGGM will be in an inclined controlled orbit of 65–70 deg at approximately 400 km altitude.

According to the NGGM Mission Requirement Document (NGGM MRD 2023), NGGM has the aim to "extend and improve time series of satellite gravity missions by providing enhanced spatial and temporal resolution time-varying gravity field measurements with reduced uncertainty and latency to address the international user needs as expressed by IUGG and GCOS and demonstrate operational capabilities relevant for Copernicus."

On ESA side, the NGGM/MAGIC concept was investigated in two parallel industry Phase A studies, and was complemented by this "NGGM/MAGIC – Science Support Study during Phase A". The main results of the first phase of the Science Support Study were already reported, see: https://www.asg.ed.tum.de/iapg/magic/documents/. Additional invesitgations were performed in a Phase A extension of 8 months. The main results and conclusions of this extension phase are summarized in this document.

The majority of the numerical simulations and impact studies were based on the baseline constellation 5d_397_70, which has the following key parameters:

Satellite	Semi-major axis [m]	Eccentr.	Incl. [°]	Asc. node [°]	Arg.of perigee [°]	Mean anomaly [°]
P1-A	6871210.979	0.0016	89	359.98	27.78	331.51
P1-B	6871208.124	0.0016	89	359.98	29.17	331.95
P2-A	6780418.955	0.0008	70	2.34	5.46	353.82
P2-B	6780416.219	0.0008	70	2.34	8.46	352.68

Generally, two noise scenarios have been investigated in either scenario – product-noise-only (PO) and full-noise (FN). In case of PO, all time-variable gravity signal components are disregarded, and only the LOS-projected noise of individual instruments is considered as an error contributor to the low-low observations. Here, we consider only the two most dominant instruments – the ACC (SuperSTAR-type for P1, MicroSTAR-type for P2) and the LRI (for P1), or LTI (for P2), respectively (see Figure 1). Further, tone errors, i.e. sinusoidal errors occurring at multiples of the orbital frequency, are considered. In case of FN, also the temporal variations of the gravity field in the form non-tidal atmosphere/ocean (AO) background model errors and ocean tide (OT) model errors are considered in addition.

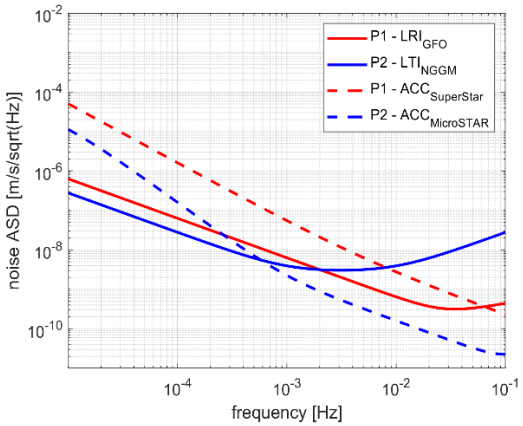

Figure 1: Product noise specification (in terms of LOS projection) for 5d_397_70.

1) L2 algorithmic development

In the frame of this project, improved processing strategies for the optimum exploitation of NGGM/MAGIC data have been developed, implemented, numerically analyzed and compared to the performance of the baseline strategy.

a) Stochastic modelling of background model errors

After a successful study on the inclusion of stochastic models of ocean tide (OT) background model errors in the first phase (Abrykosov 2022b), in the extended phase we concentrated on the stochastic modelling of non-tidal atmosphere and ocean (AO) background models. It could be demonstrated that already a static error variance-covariance matrices (VCM) is beneficial for the reduction of aliasing stemming from AO errors, see Figure 2 (left), where different variants have been investigated. The investigation of time-variable VCMs was started, but is not yet successful (Figure 2, right) and is still work in progress.

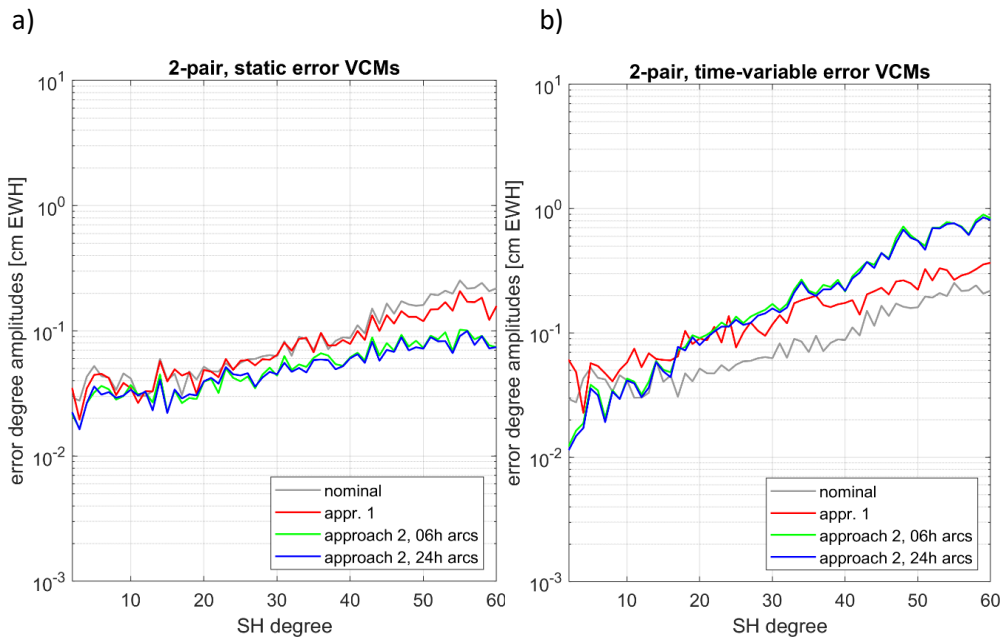

Figure 2 Retrieval errors when using a) static AO error VCM, and b) time-variable error VCMs for different approaches.

b) Extended parameterization schemes

The performance of the DMD approach (Abrykosov et al. 2022a) in the frame of a double-pair-based gravity retrieval, was carried out on the basis of observation geometry of the baseline scenario 5d_397_70. It could be shown that the DMD approach has some advantages over the alternative "Wiese approach (Wiese et al. 2011). Especially in the case of very different relative weights of P1 and P2 due to the altitude difference and different instrumentation, the underlying normal equation system of the DMD is more stable. The DMD was also investigated for its potential to apply multiple sequential short-term estimates before solving for final, e.g. monthly, gravity products, and showed very promising results (Figure 3).

The approach has to be seen in context with stochastic modelling of OT BM errors described in a). It indeed offers an added value, as it allows to utilize the benefit of both methodologies, but several effects still have to be studied in further detail.

a) b)

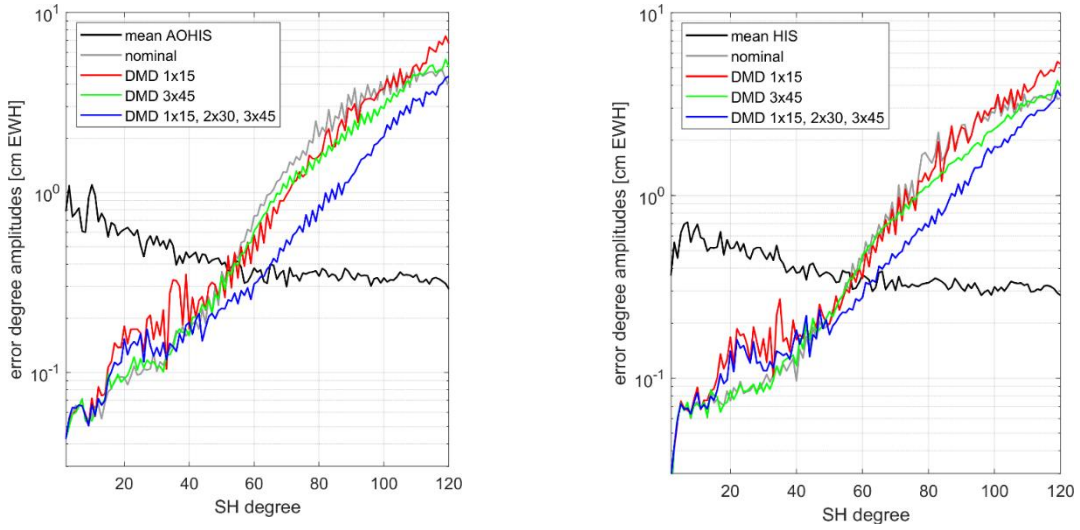

Figure 3: Retrieval errors of the 30-day estimate obtained with various DMD parametrization schemes. a) Retrieval of the full AOHIS; b) retrieval of HIS (i.e. a priori BM-based AO de-aliasing is applied).

c) Treatment of P1 – P2 transition zone artefacts

This WP was triggered by an open issue of the first phase: It was identified that in the double-pair solutions (based on a different scenario 3d_H), the polar regions which are only covered by the polar pair (P1) are sometimes degraded compared to the polar single-pair solutions. The tailored spherical cap regularization strategy (Metzler and Pail 2005), which constrains the double-pair solutions towards to P1-solution in the polar cap areas, without changing the solution in the regions covered by both pairs ($|\varphi| < 70°$) significantly, was modified and adapted to the current baseline scenario 5d_397_70, and a second comparable approach in space domain was implemented. Both approaches succeed to constrain the double-pair solution towards the polar pair in the polar areas (Figure 4). However, the single-pair solution is not always superior to double-pair in polar cap areas, so that it is difficult to define a generalized strategy. It is recommended to apply a weak regularization towards polar-pair solution.

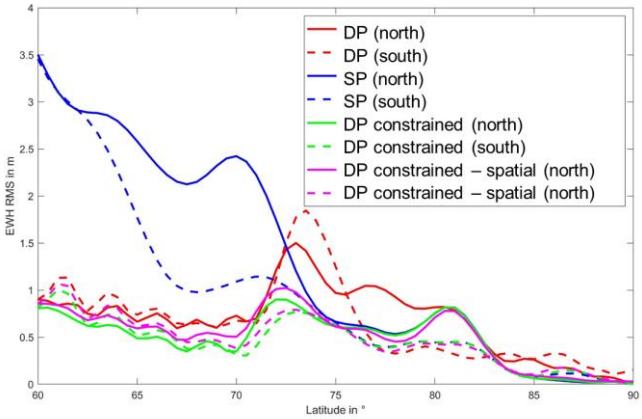

Figure 4: EWH RMS per latitude for baseline scenario 5d_397_70: constraints toward single-pair solution applied in spectral and spatial domain.

d) HIS vs. AOHIS estimation

The nominal and the DMD method were applied to the 5d_397_70 scenario either with on-the-fly AOD1B de-aliasing, or without de-aliasing, followed by a posteriori subtraction of AO+AOerr. They show very similar results (Figure 5). It is recommended to provide users with both a HIS and an AOHIS product. The nominal method will deliver the HIS signal, while the DMD method will result in the full AOHIS signal.

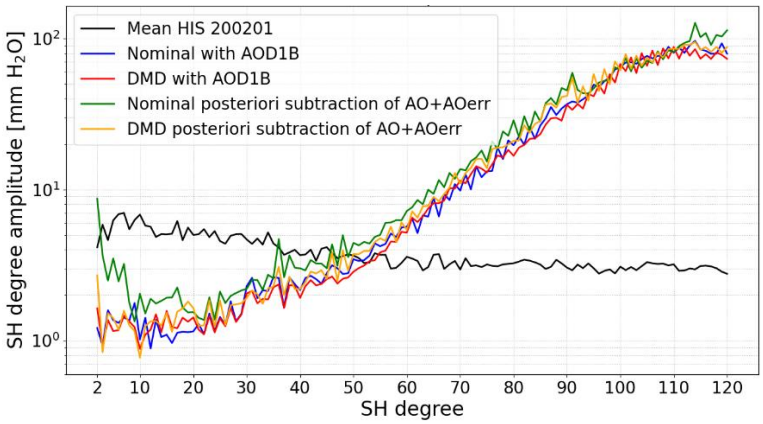

Figure 5: Degree (error) amplitudes of various scenarios to evaluate HIS vs. AOHIS estimation.

e) Bump at around degree 80 in TUM full-noise 31-day solution

The monthly P1+P2 and P2-only 5d_397_70-based full-noise solutions of TUM have been shown to feature a “bump” in the spectral range between d/o ca. 75 and 90 (c.f. Figure 6). Upon further investigation, it was also determined that the “bump” occurs in the same manner regardless of the chosen resolution of the estimated field as well as regardless of the underlying time interval over which the field is estimated (provided the respective solution’s intrinsic noise level is sufficiently low). It could ultimately be shown that the bump originates from the observation geometry coupled with the sampled time-variable signal, and can to a large extent be regulated by means of the applied co-

variance matrix of observation errors. The stochastic modelling is very likely also the reason why the GFZ solutions do not feature a similar bump, as it is applied differently at TUM and GFZ.

The stochastic modelling in the nominal processing scheme was for now based exclusively on the specifications of the instrument noise. Due to the presence of time-variable gravity signal components in the observations, however, this method is, in a strict sense, flawed. Therefore, tweaking the observation VCM in a way that yields an optimal result cannot be regarded as incorrect either. However, an improved stochastic modelling is recommended for use in the future which takes into account the stochastics of all observation components. This concerns specifically the AOD and OTD background model errors in addition to the instrument noise as the most dominant error contributors. This "complete" stochastic modelling is expected to produce optimally tailored weighting to the respective set of observations, and to directly solve the issue of relative weighting between observations of different satellite pairs.

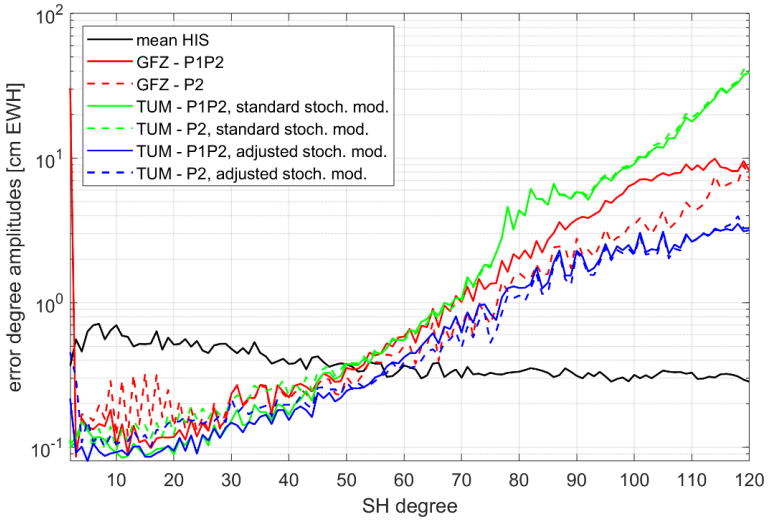

Figure 6: Comparison of monthly full-noise solutions produced by TUM and GFZ on the basis of the 5d_397_70 observation geometry.

f) Fast-track processing strategy

A functional fast-track (NRT) retrieval scheme on the basis of a sliding window approach was already developed by Purkhauser and Pail (2019). This method was adapted by applying the DMD parametrization scheme instead of the Wiese approach, which facilitates the retrieval of gravity products over shorter time scales. In turn, this allows for a reduction of the latency time at which variations in temporal gravity can be computed, as comparisons can already be carried out on the basis of interval (de-aliasing) products. Evidently, the clear drawback is that a shorter latency also results in a reduced spatial resolution. However, there is freedom to compute interval fields over – in principle – arbitrary time intervals, which allows a better tailoring of the retrieval scheme to the user groups' requirements regarding latency times.

2) P2-only solutions

The performance of solutions which are only based on the inclined pair (P2) of the baseline scenario 5d_397_70 was evaluated. In order to account for the lack of observations in the polar regions, a spherical cap regularization (Metzler and Pail 2005) was applied for the regions $|\varphi|>70°$.

Due to the polar gaps, global metrics like degree error amplitudes do not work anymore, at least not without modifications. Therefore, it is recommended to assess the performance in the spatial domain, e.g. in terms of grids of equivalent water height difference, limited to the regions that are covered by the inclined pair.

Figure 7 shows a comparison of the performance of the P2-only and the P1+P2 solution. It clearly demonstrates that the performance in those areas covered by P2 is dominated by P2. The relative contribution of P2 to the total P1+P2 solution is about 97%.

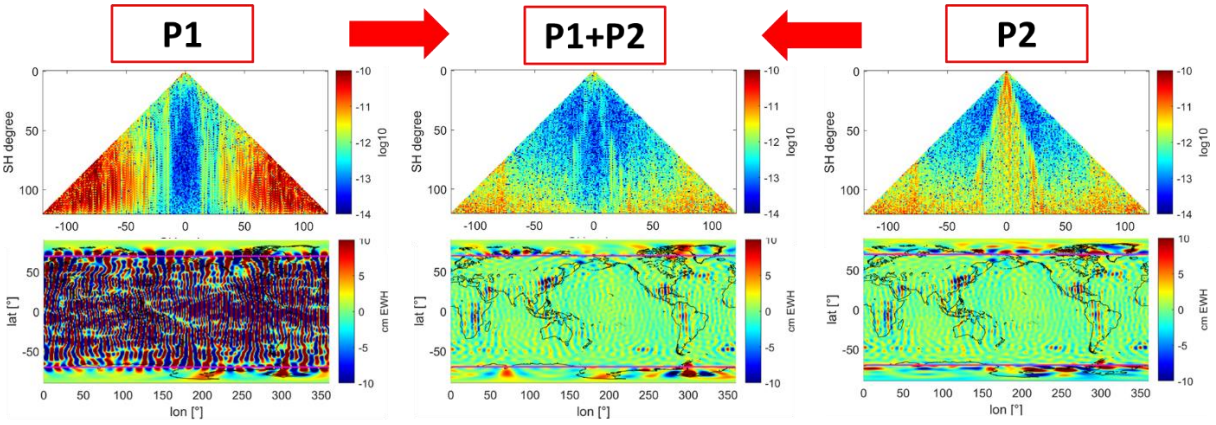

RMS [EWH] for $|\varphi| < 70°$

cm [EWH]	P1	P1+P2	P2
d/o 60	18.47	1.79	1.83
d/o 90	389.68	19.74	20.15

Figure 7: Coefficients (top row), EHW differences up to SH degree 60 (middle row) and key statistics of P1, P2 and P1-P2 constellations based on baseline scenario 5d_397_70.

Regarding co-estimation of daily parameters applying the Wiese approach, the reduced spatial resolution of a single-pair P2 solution does not allow for similar retrieval quality as in P1+P2 scenario when evaluated to a max. spherical harmonic (SH) degree of 15, but still the P2-only solution performs much better than the polar pair P1-only solution. However, when reducing the max. SH degree to 10, the P2-only solution is competitive with the double-pair P1+P2 solution (Figure 8).

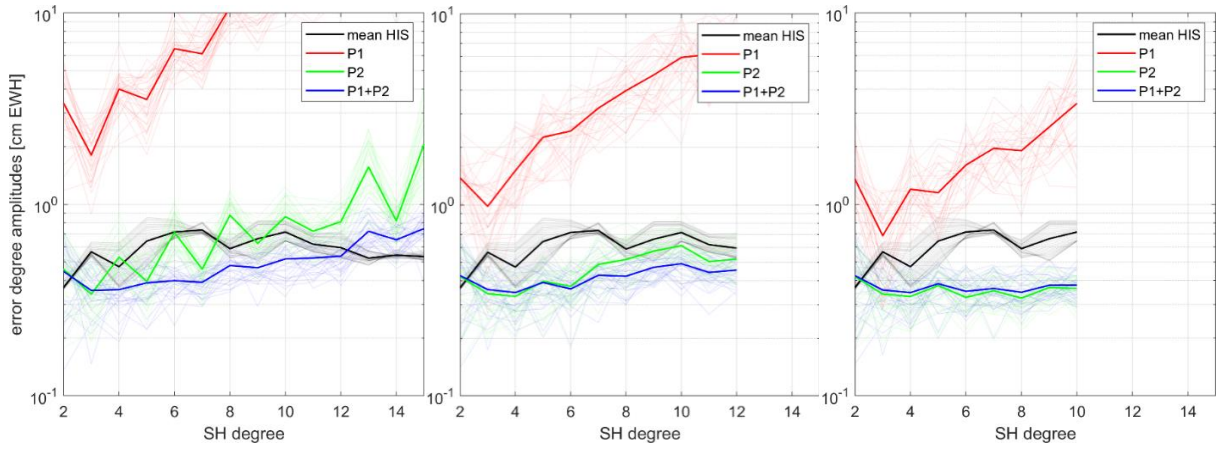

Figure 8: Daily "Wiese" co-estimates with maximum SH degree a) 15, b) 12 and c) 10, for P1-only, P2-only and P1+P2 constellations.

3) Match against NGGM MRD requirements

All simulation scenarios performed in this study were evaluated in terms of cumulative EHW errors, and the results were compared against the NGGM MRD requirements (NGGM MRD 2023). The results are depicted in Figure 9 for P2 and in Figure 10 for P1+P2, respectively. Note that these were obtained with the optimal stochastic modelling (c.f. section 1.e).

In case of P2, all threshold requirements can be met fully for the 31-day retrieval. In case of the 5-day retrieval, only the threshold requirement for d/o 2 is missed.

In case of P1+P2, the threshold requirement for d/o 10 is just barely missed for the 31-day retrieval, while all others are met. For the 5-day retrieval, just like in case of P2-only, the threshold requirement at d/o 2 is not met. Additionally, the requirement at d/o 10 is just barely missed.

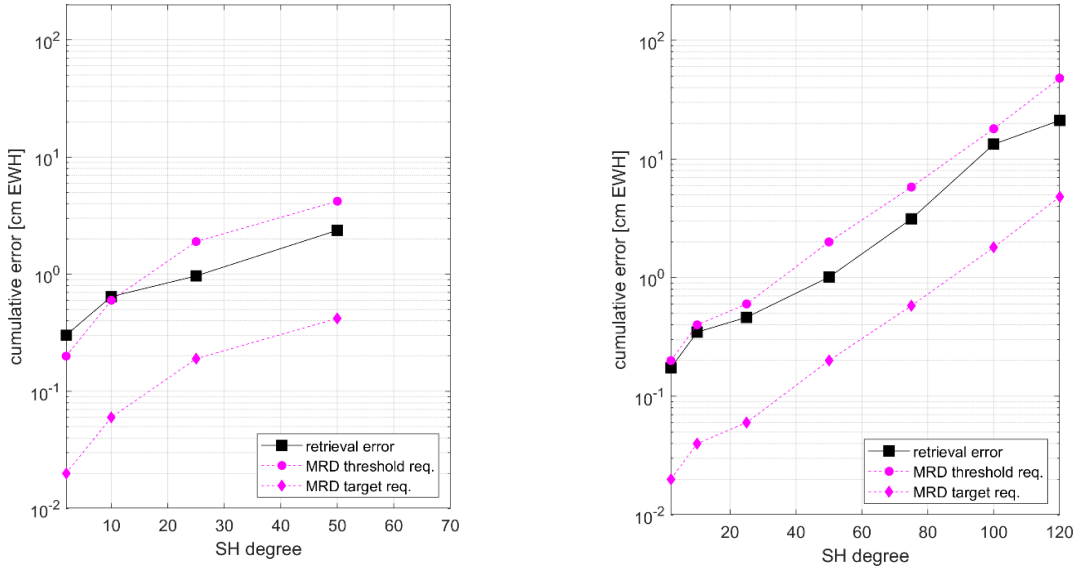

Figure 9: Mean cumulative spatial error of 5-day (left) and 31-day (right) P2-based solutions evaluated in the latitude range [-70°,70°] and compared against the NGGM Level-2a requirements.

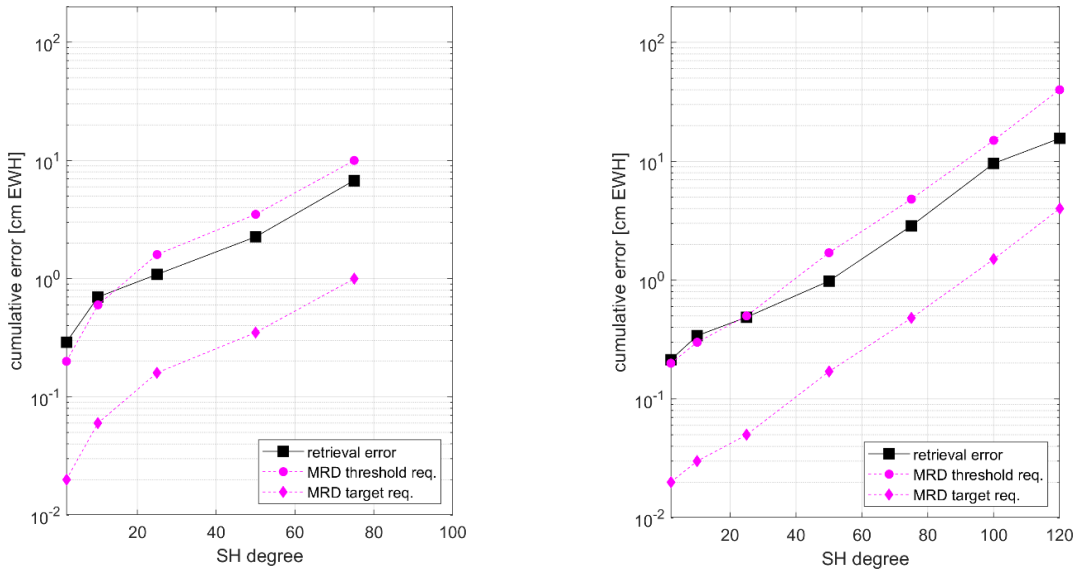

Figure 10: Mean cumulative spatial error of 5-day (left) and 31-day (right) P1+P2-based solutions evaluated in the latitude range [-90°,90°] and compared against the MAGIC Level-2a requirements.

4) 3rd numerical simulator implementation at CNES

A third numerical simulator based on the GINS software was implemented at CNES. Closed-loop simulation results based on the baseline scenario 5d_397_i70 were compared against GFZ solutions and show similar results. Numerical problem with the stochastic modelling of product errors were solved toward the very end of the project. In summary, the development CNES simulator has made very good progress during this extended project phase, but it has not yet reached the same degree of maturity as the GFZ and TUM simulators.

5) Scientific impact analysis

The science impact analysis carried out in CCN1 in different fields of Earth Sciences revealed a strong benefit of the NGGM and MAGIC constellations over a polar-pair only GRACE-like mission. NGGM and MAGIC perform similarly well in most evaluation cases. This is shown exemplarily in terms of the root-mean-square difference (RMSD) for 405 river basins for a spatial resolution of 400 km in Figure 11.

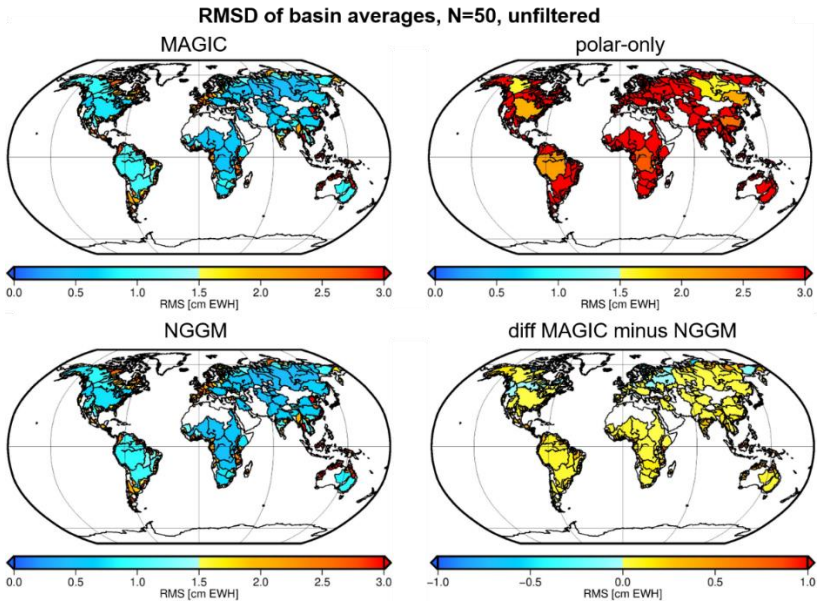

Figure 11: Temporal RMSD of 5-days simulation output and reference solution truncated at N=50 for basin averaged time series of 405 river basins defined by the Global Runoff Data Center (GRDC): double-pair MAGIC mission (top left), polar-pair-only (top right) and NGGM (bottom left). The figure on the bottom right shows the difference between the MAGIC and the NGGM result.

For water storage variations in river basins, the scenarios with 5-day resolution largely fulfil the envisaged mission performance for short-term mass variations in hydrology. This similarly applies to the detection of wet and dry extremes of water storage anomalies at the level of individual 5-day intervals. While a polar-pair scenario is dominated by false positive alerts for extreme events, i.e., the exceedance of wet or dry thresholds while there is no such event, the lower noise of NGGM and MAGIC largely improves the ratio of correctly versus incorrectly detected hydrological extremes.

The accuracy of glacier mass change observations increases by orders of magnitude at mid latitudes, both a short and long time scales. As an example, Figure 12 shows a performance evaluation for a 12-year simulation. The noise level at the mid-latitude regions (Arctic Canada South, Iceland, and Southern Andes) is reduced by one order of magnitude when adding an inclined satellite pair. At higher latitudes,

the double pair constellation still outperforms the single pair in all regions, although the noise reduction is less substantial. To which extent NGGM threshold or target requirements for can be met for these glacier mass change applications depends on the considered spatial resolution and on the region.

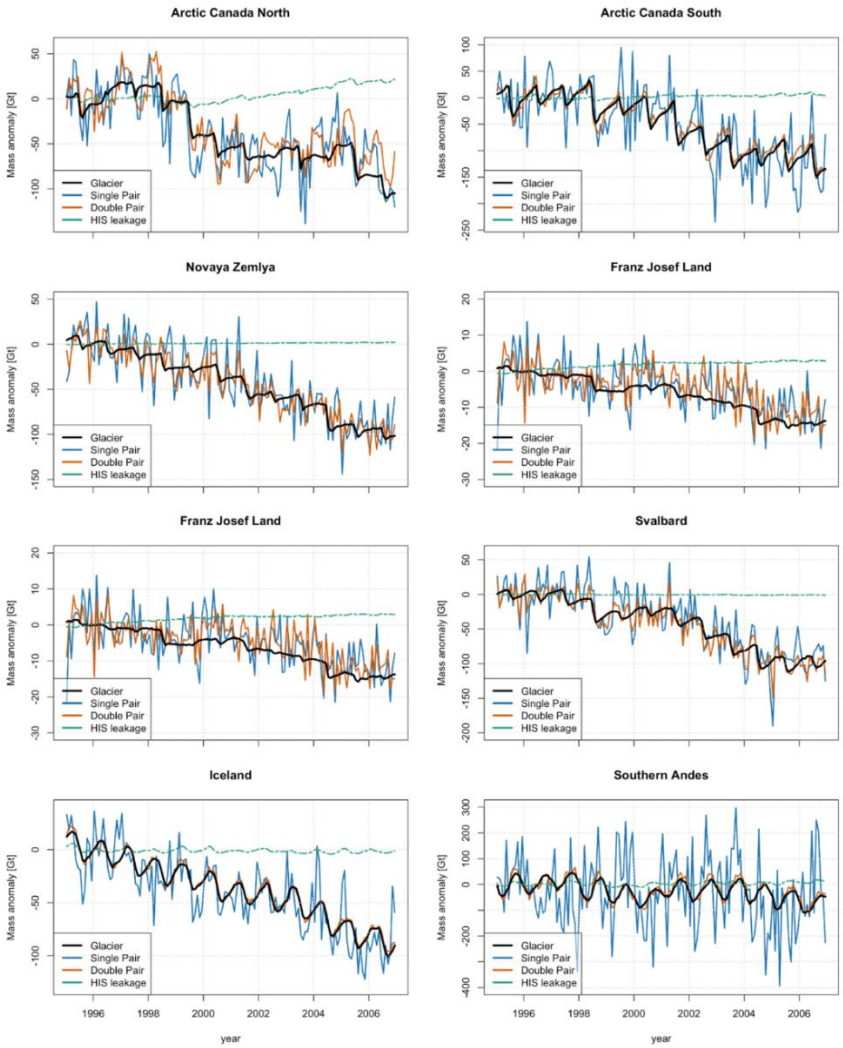

Figure 12: Time series of mass variations in glacier regions retrieved from the 12-yr closed loop simulations for a single (blue) and dual (orange) pair mission concept. The green lines show the leakage signal from non-glacier components in the HIS model.

Furthermore, a dual-pair satellite configuration is shown to be able to detect 5-year running mean AMOC changes with an accuracy level that is comparable with (and independent of) the best in-situ measurements and thus is of great value for ocean climate monitoring. Figure 13 shows the actual model AMOC in the North Atlantic between 25°N and 45°N (black) and its reconstruction (blue) using the ideal simple weighting function. Very good agreement can be achieved for 5-year means or longer). Figure 15 shows the related noise calculations, with the upper panels representing the actual time series of erroneous AMOC from fields truncated at degree 90, and the lower panels giving summary statistics for the same cases at different truncations. In panels a-e, black is for monthly values, blue for running annual mean, and pink for running 5-year mean. Thin lines (except the black lines in b) and c)) are single-pair noise, thick lines for double-pair noise, and dots for signal leakage. It is clear that the dual-pair noise is substantially below that for a single pair. The degree 90 truncation is the worst case for the single pair in this comparison, but comparing thick and thin lines with matching colours in

Fehler! Verweisquelle konnte nicht gefunden werden.d shows that this is the case at all truncations (note the logarithmic scale). Although the double-pair configuration produces noise below 1 Sv for a wide variety of truncations, for annual and 5-year mean time series, this is somewhat academic as the leakage signal is much higher over most of this range. While the measurement noise increases towards degree 90, the leakage noise decreases, and the optimal retrievals occur where the best compromise is found. For 5-year means, this is at about degrees 75-90, and gives RMS errors of about 0.4 Sv from each source (0.6 Sv total if added in quadrature).

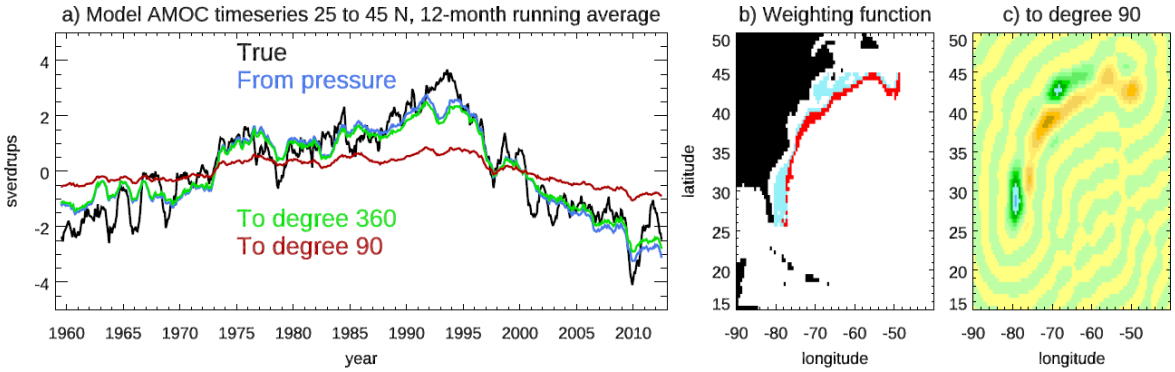

Figure 13: AMOC and its reconstruction from boundary pressures in the 1/12 degree resolution NEMO ocean model: a) The true model AMOC (black), its reconstruction using pressures with the best, simple weighting function (blue), and when the pressure data are truncated at degree 360 (green) and 90 (red). b) simple weighting function used. c) simple weighting function truncated at degree 90.

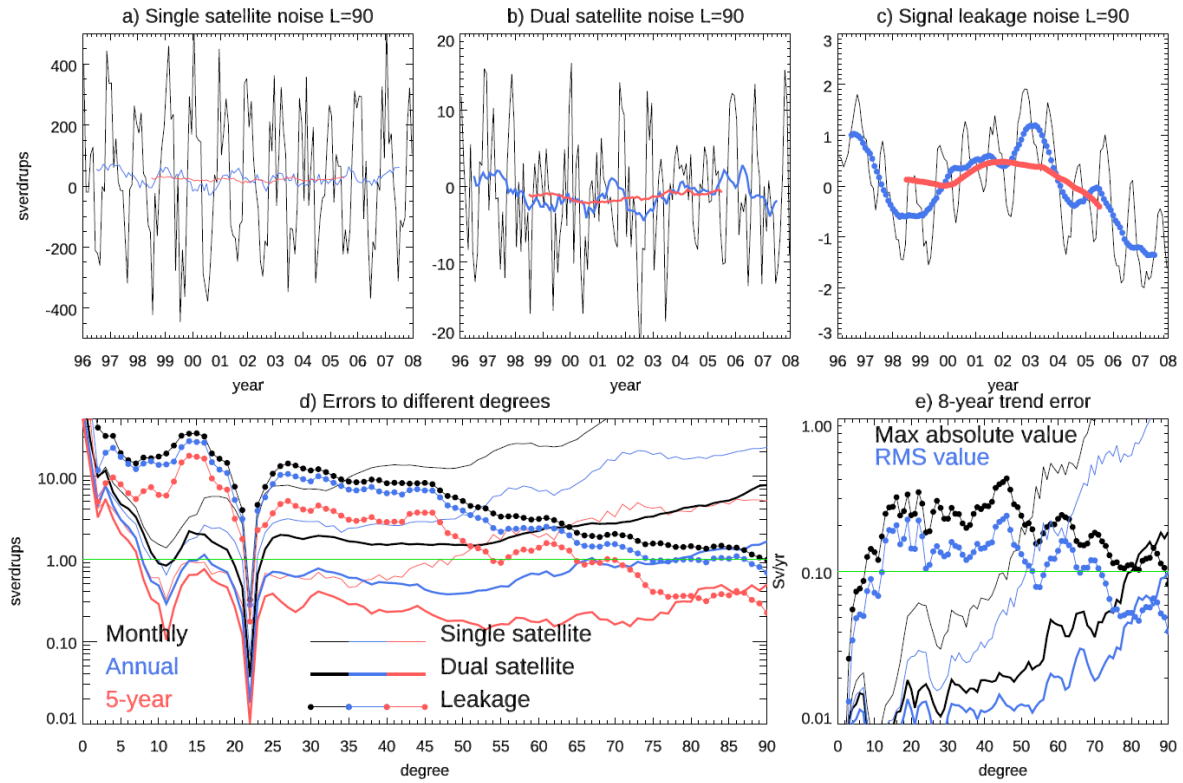

Figure 14: Noise in the pressure-predicted AMOC retrieval under different observation scenarios. a) measurement noise in a single pair scenario, showing monthly values, running annual means, and running 5-year means for a retrieval truncated at degree 90. b) as for a), but using a two-pair scenario. c) leakage effects due to truncation for the "truth" model. d) Standard deviations of the above time series, but for different truncations. e) maximum absolute value and rms value of linear trends fitted to all 8-year subsets of the three noise time series, with no smoothing. Thin lines represent single-pair noise, thick lines for double-pair, and dots for leakage.

For detecting earthquake signals, NGGM and MAGIC perform greatly better than the polar only pair, with added value in observing the co-seismic and the post seismic signal. Figure 15 shows the sensitivity of single- and double-pair missions regarding the detectability of the co-seismic gravity signal of selected big earthquakes.

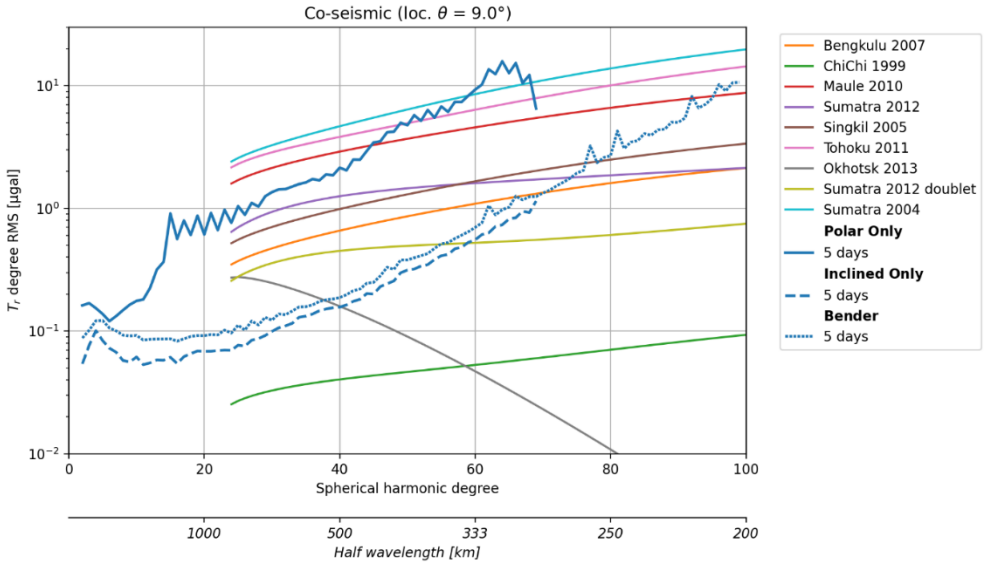

Figure 15: Error degree amplitudes of the MAGIC mission scenarios: polar only, inclined only and Bender double-couple and the signal degree amplitudes (localized) of the coseismic signal for selected earthquakes. 5-day time integration for the gravity acquisition at the satellite.

The value of an AOHIS product that is directly estimated from the gravity observations is considered to be low for atmospheric mass estimates over the continents, whereas it is deemed potentially useful for several oceanographic analyses. For long time scales (longer than about 1-month period), the comparison of AOHIS and HIS products will enable the quantification of the dealiasing error using external dealiasing models at these long timescales. For shorter timescales, current methods use a remove-restore technique based on ocean models, with GRACE providing additional information via filters/regularizations worked out in a number of different ways by different groups. When comparing with observations, this makes it very difficult to assess how much explained variability is due to GRACE and how much due to the prior models. An independent AOHIS product is very valuable for testing and developing models of global-scale processes on such time scales, particularly around 5-day period, which, although small in amplitude (typically a few cm at most), have the potential to play an important role in storm surge predictions for flooding, and in determining the ocean's contribution to earth rotation.

Specifications of an NRT/fast-track mass change product that can satisfy a large part of related applications and services are summarized from user surveys and literature to be of 5-day temporal resolution with daily updates and a maximum latency of 2 days.

The processing of acceleration measurements to density and crosswind observations is well-established. Such observations constitute a valuable data set for use in thermospheric density and wind modeling and related applications. A roadmap has been formulated for establishing this processing and usage. This includes the generation of density and crosswind data products (Level 2). In a fast-track processing chain, where very short latencies of max. 12-14 hours are required for operational service applications. The Level 2 density data product generated with minimum latency can be assimilated into empirical and physics-driven thermosphere models (e.g., TIE-GCM; Level 3).

More relaxed latency requirements apply for several scientific applications, such as the validation of thermosphere models or even the assimilation of density observations into these models, and studying dynamics during geomagnetic storms.

Based on these studies on various application fields, adaptations of the user requirements of the NGGM MRD were proposed.

6) L0-L1b inter-satellite distance algorithm development

A novel processing chain to simulate Level-0 LTI ranging data from orbit simulation inputs was implemented, and the underlying methodology was documented in detail (Figure 16). The generated data is then further processed to Level-1a and Level-1b.

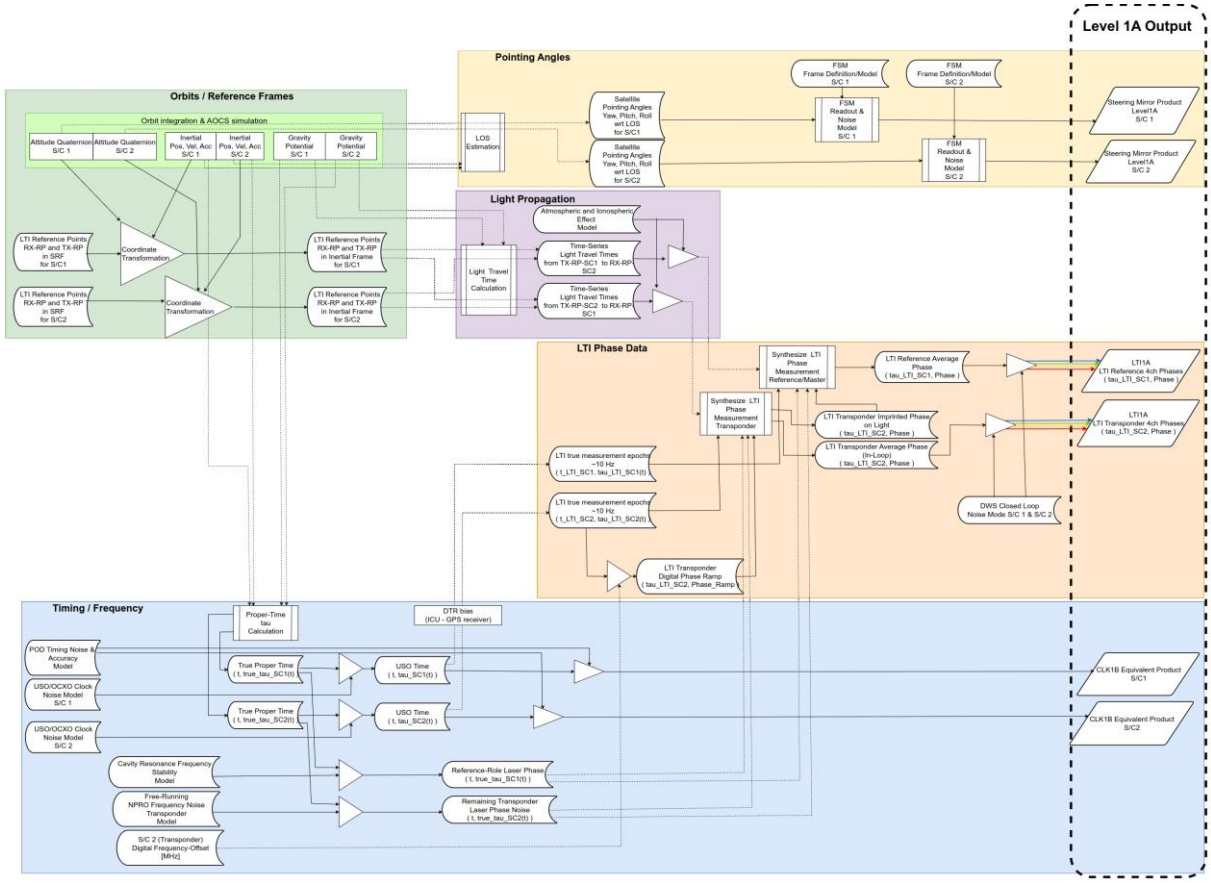

Figure 16: Flowchart for the generation of realistic LTI Level-0/Level-1a data.

A first simple Level1a and 1b product was derived, which used a few simplifications and noise-free assumptions. Furthermore, this dataset was limited by a non-optimal interpolation method. In a more realistic dataset, the interpolation method was improved to obtain a lower noise for the orbit data and light travel times. Also different noise models, such as USO noise, POD noise and laser frequency noise, were included in the simulations.

For the next versions of the simulator, the missing parts from the flowchart will be implemented, namely:

- Light travel time calculation between TX and RX reference points

- TTL and ARC simulation (insert offset in reference points)
- consider remaining transponder laser phase noise (due to finite gain of the transponder lock)
- use attitude quaternions and corresponding orbits in inertial frame from the mission primes
- consider atmospheric and ionospheric effects in light travel time calculation
- consider a noise model for DWS closed loop
- consider noise for FSM readout when generating pointing angle products
- consider a phase readout noise (1µcycle/√Hz)

Though the simulator was intended primarily to derive LTI Level-1a data, it was already now in the early state extremely useful to better understand, validate and improve the Level-0 to Level-1b processing chain of LTI/LRI data, because this novel simulator uses a completely different approach and is not just reverting the processing steps of the existing Level-1a to Level-1b processing chain.

7) In-orbit accelerometer calibration

GNSS-based accelerometer calibration allows for a very precise determination of accelerometer biases for the X axis (predominantly the flight direction): precisions much better than 0.1 nm/s^2 are feasible when using the full error model. For the Y and Z axes (predominantly in the cross-track and height direction, respectively), these precisions are typically better than 1 and 4 nm/s^2, respectively. Of the error sources investigated, uncertainties in the tide model and uncertainties/omissions in the temporal gravity field model (e.g., errors in the de-aliasing models) are the dominant ones. The latter might be mitigated by co-estimating the gravity field.

The capability of GNSS-based accelerometer calibration for estimating accelerometer observations strongly depends on the magnitude of the (residual) non-gravitational accelerations. Four scenarios have been investigated based on the possible combinations of flying during solar minimum or maximum on the one hand and flying 1D or 3D drag free control (DFC). In case of 3D DFC, no reliable estimation of accelerometer scale factors is feasible. In case of 1D DFC, where the DFC is aligned with the X axis, only reliable scale factors for the Y and Z axes can be estimated with precisions ranging between about 0.001 and 0.18 nm/s^2 for the Y axis and 0.001 and 0.04 nm/s^2 for the Z axis. Better precisions are obtained for the solar maximum period, when the 1D DFC leaves bigger non-gravitational accelerations. During solar minimum, the uncertainty of the estimated scale factors is about 10 times worse than during solar maximum. Especially for the Y axis, the TASI simulations display a decreasing trend of the order of magnitude of the residual accelerations, leading to larger errors in the retrieved Y axis accelerometer scale factors.

Including the LRI observations in the POD-based accelerometer calibration, i.e., together with the GNSS-estimated orbit coordinates, might lead to a degraded estimation of accelerometer calibration parameters. Finding the optimal relative weight of the GNSS and LRI observations is not straightforward. Remaining gravity field modeling errors (as in, e.g., the de-aliasing products) have a relatively big impact on the LRI observations as compared to the GNSS observations. This is a contributing factor to less precise accelerometer calibration parameter estimates, despite the very high precision of the LRI observations themselves.

8) Documentation of ground processing algorithms and Science Readiness Assessment

The ground processing algorithms of the involved project partners TU Munich, GFZ and CNES were documented in an Algorithm Theoretical Basis Document (ATBD) for Level-1a to Level-3, and corresponding Science Readiness Levels (SRL) were assigned, following the criteria defined in the SRL

Handbook. Since NGGM is at the end of Phase A extension, according to the SRL Handbook the SRL to be achieved is SRL-5, indicating a successful assessment of the Mission Performance with the Delta-Preliminary Requirements Review (D-PRR). SRL5 was assessed in the frame of a Science Readiness Assessment (SRA).

It could be demonstrated that the performance simulators at TUM and GFZ have reached a high degree of maturity and can provide robust and reliable results. This reliability is further strengthened by the fact that the two independent simulation environments can be used to validate each other. The involved algorithms applied for the baseline processing scheme have an SRL which is generally at least 5, but in many cases even higher than 5.

9) Evaluation of various drag-free scenarios in interaction with industry

Five product-noise scenarios representing various drag-compensation scenarios were simulated and provided by TASI. These scenarios differ by the amplitudes of assumed non-gravitational forces as well as their compensation – the ID components MIN and MAX denote the assumption of minimum or maximum level of expected drag, while the 3D and 1D components indicate whether the drag compensation is carried out in all three spatial directions or just in along-track direction.

The impact of these product noise scenarios on the performance of L2 gravity products has been investigated within a product-noise only and a full-noise (i.e. temporal gravity signal in addition to product noise) 5-day retrieval based on a stand-alone P2. The results presented in Figure 17 indicate that the level of drag compensation only notably affects the retrieval if the temporal gravity signal is disregarded. Once the temporal signal is added, however, it dominates the retrieval performances, while the observation errors stemming from the various drag scenarios are negligible.

10) Outreach – scientific papers

The main results of the first phase of the MAGIC Phase A Science Support Study were documented in two scientific papers:

- Heller-Kaikov B., Pail R., Daras I. (2023), Mission design aspects for the mass change and geoscience international constellation (MAGIC). Geophys. J. Int. 235(1): 718–735, https://doi.org/10.1093/gji/ggad266.
- Daras I., March G., Pail R., Hughes C.W., Braitenberg C., Güntner A., Eicker A., Wouters B., Heller-Kaikov B., Pivetta T., Pastorutti A. (2023). Mass-change And Geosciences International Constellation (MAGIC) expected impact on science and applications. Geophys. J. Int., in review (status: October 2023).

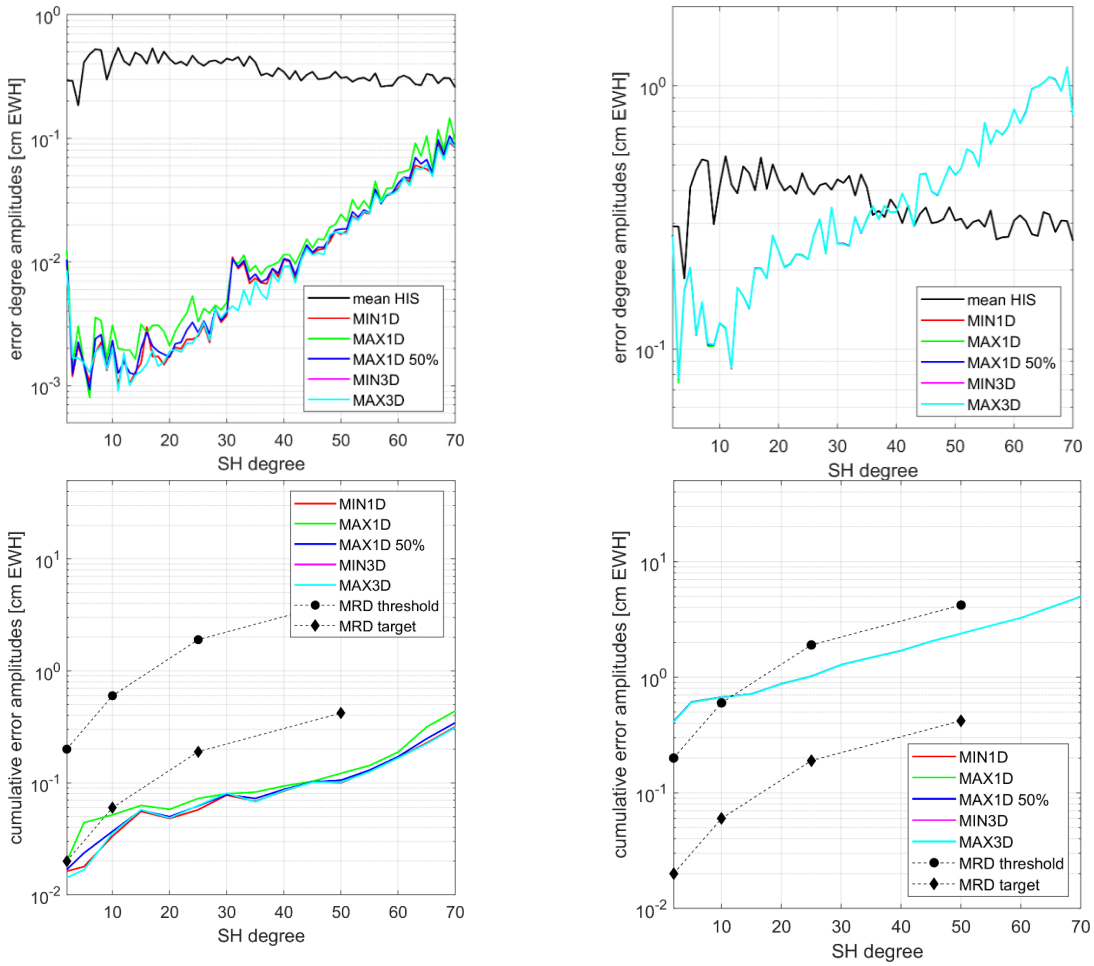

Figure 17: Impact of drag compensation on the performance of gravity field retrieval in terms of degree ampliutudes (top row) and cumulative errors (bottom row, evaluated in the spatial domain for observation-covered regions). Note that the "polar gap wedge", i.e. the coefficients affected by the polar gaps, have been removed in the degree amplitudes for better comparability. Left – product-noise-only simulation scenario, right – full-noise simulation scenario.

References

Abrykosov P., Murböck M., Hauk M., Pail R., Flechtner F. (2022a): Data-driven multi-step self-de-aliasing approach for GRACE and GRACE-FO data processing, Geophysical Journal International, ggac340, doi: https://doi.org/10.1093/gji/ggac340.

Abrykosov P., Sulzbach R., Pail R., Dobslaw H., Thomas M. (2022b): Treatment of ocean tide background model errors in the context of GRACE/GRACE-FO data processing. Geophysical Journal International 228 (2022). 1850-1865, doi: https://doi.org/10.1093/gji/ggab421.

Hauk M., Pail R. (2018): Treatment of ocean tide aliasing in the context of a next generation gravity field mission. Geophysical Journal International 214, 345-365, doi: https://doi.org/10.1093/gji/ggy145.

Metzler B., Pail R. (2005): GOCE Data Processing: The Spherical Cap Regularization Approach. Studia Geophysica et Geodaetica 49(4): 441–462, doi: https://doi.org/10.1007/s11200-005-0021-5.

MRD (2020): Mission Requirements Document, Next Generation Gravity Mission as a Mass-change And Geosciences International Constellation (MAGIC) - A joint ESA/NASA double-pair mission based on NASA's MCDO and ESA's NGGM studies. ESA-EOPSM-FMCC-MRD-3785.

NGGM MRD (2023): Next Generation Gravity Mission (NGGM): Mission Requirements Document. Issue 1.0., ESA-EOPSM-NGGM-MRD-4355, ESA Earth and Mission Science Division.

Pail R., Bingham R., Braitenberg C., Dobslaw H., Eicker A., Güntner A., Horwath M., Ivins E., Longuevergne L., Panet I., Wouters B. (2015): Science and User Needs for Observing Global Mass Transport to Understand Global Change and to Benefit Society. Surveys in Geophysics, 36(6):743-772, doi: https://doi.org/10.1007/s10712-015-9348-9.

Purkhauser A.F., Pail R. (2019). Next generation gravity missions: near-real time gravity field retrieval strategy. Geophys. J. Int. 217(2), 1314–1333, https://doi.org/10.1093/gji/ggz084.

Wiese D.N., Visser P., Nerem R.S. (2011): Estimating low resolution gravity fields at short time itnervals to reduce temporal aliasing errors. Advances in Space Research 48 (2011), 1094-1107, doi: https://doi.org/10.1016/j.asr.2011.05.027.